GENETICS

10.1126/sciadv.1501031

Large-scale diversification without genetic isolation in nematode symbionts of figs

Vladislav Susoy,[1] Matthias Herrmann,[1] Natsumi Kanzaki,[2] Meike Kruger,[3] Chau N. Nguyen,[4] Christian Rödelsperger,[1] Waltraud Röseler,[1] Christian Weiler,[1] Robin M. Giblin-Davis,[5] Erik J. Ragsdale,[6]* Ralf J. Sommer[1]*

Diversification is commonly understood to be the divergence of phenotypes accompanying that of lineages. In contrast, alternative phenotypes arising from a single genotype are almost exclusively limited to dimorphism in nature. We report a remarkable case of macroevolutionary-scale diversification without genetic divergence. Upon colonizing the island-like microecosystem of individual figs, symbiotic nematodes of the genus *Pristionchus* accumulated a polyphenism with up to five discrete adult morphotypes per species. By integrating laboratory and field experiments with extensive genotyping of individuals, including the analysis of 49 genomes from a single species, we show that rapid filling of potential ecological niches is possible without diversifying selection on genotypes. This uncoupling of morphological diversification and speciation in fig-associated nematodes has resulted from a remarkable expansion of discontinuous developmental plasticity.

INTRODUCTION

Radiations of species into underused habitats are a basic generator of biological diversity, and their results can be observed at all evolutionary depths and in most groups of living organisms (*1*, *2*). A fundamental principle of diversification is that phenotypic divergence coincides with or follows lineage branching, or speciation (*3*–*5*). However, the ability of "diverging selection" to occur within species, specifically those with discrete developmental plasticity, or polyphenism, suggests that morphological divergence need not be linked to lineage diversification (*6*). This phenomenon has been mostly observed as dimorphism, whereas examples of a greater number of divergent developmental phenotypes from a single genotype are exceedingly rare, usually limited to mating types, seasonal morphs, or clonal individuals with a common ecological function (*7*–*10*).

Here, we describe a remarkable case of extreme trophic diversification uncoupled from genetic isolation by the multiplication of a developmental polyphenism. We report exaggerated variation of feeding morphs within each of seven previously unknown nematode species (Fig. 1). All of these species were found in association with figs and their pollinator wasps, with the latter being known to transmit wasp-parasitic and floret-feeding nematodes (*11*–*16*). We analyze three new nematode species that have expanded an ancestral dimorphism to establish several new morphs and trophic guilds within figs. We describe the new species as *Pristionchus borbonicus* sp. nov., *Pristionchus sycomori* sp. nov., and *Pristionchus racemosae* sp. nov. (Phylum Nematoda, Family Diplogastridae), which were isolated from the figs *Ficus mauritiana* (La Réunion Island), *Ficus sycomorus* (South Africa), and *Ficus racemosa* (Vietnam) and their agaonid pollinators *Ceratosolen coecus*, *Ceratosolen arabicus*, and *Ceratosolen fusciceps*, respectively.

[1]Max Planck Institute for Developmental Biology, Department of Evolutionary Biology, Spemannstraße 37, Tübingen 72076, Germany. [2]Forest Pathology Laboratory, Forestry and Forest Products Research Institute, 1 Matsunosato, Tsukuba, Ibaraki 305-8687, Japan. [3]Department of Genetics, University of Pretoria, Pretoria 0002, South Africa. [4]Institute of Ecology and Biological Resources, Vietnam Academy of Science and Technology, 18 Hoang Quoc Viet Road, Hanoi, Vietnam. [5]Fort Lauderdale Research and Education Center, University of Florida–IFAS, 3205 College Avenue, Fort Lauderdale, FL 33314, USA. [6]Department of Biology, Indiana University, 915 East 3rd Street, Bloomington, IN 47405, USA.
*Corresponding author. E-mail: ragsdale@indiana.edu (E.J.R.); ralf.sommer@tuebingen.mpg.de (R.J.S.)

RESULTS

Extreme disparity of forms in an island-like microecosystem

Initial observations indicated that *Pristionchus* nematodes associated with figs show a high degree of morphological variation among adult forms, especially in their feeding structures. To determine the extent of this variation, we examined hundreds of nematode individuals and uncovered five distinct morphotypes associated with each of the three fig species mentioned above. Morphs associated with a single fig species differed qualitatively in their mouthpart complexity, or the total number of spatially independent structures or "cusps" arising from the nematode stoma (*17*), including the presence and number of movable teeth, serrated plates, and labial appendages (Figs. 1 and 2A). Furthermore, the shape and size of mouthparts for different morphs were strikingly disparate. Specifically, principal components analysis (PCA) of the geometric morphometrics of mouth shape and form (the latter including landmark-derived shape data + log centroid size) (*18*, *19*) showed the five morphs in each fig species to occupy different parts of Procrustes morphospace with no or little overlap in shape, form, or both (Fig. 2B). Overall, the degree of discontinuous morphological variation that we observed between individuals from figs exceeded that observed between nominal genera of the same family (*17*) and among all other examined species of *Pristionchus* combined (Fig. 3), with some morphs exhibiting fantastic structures that, to our knowledge, have no analogs in other known nematodes (Figs. 1, C and E, and 2A).

Morphological diversity from single genotypes

Despite the disparity of adult nematode morphotypes discovered in individual figs, we surprisingly found that all *Pristionchus* nematodes isolated from a given fig species always had identical 18*S* ribosomal RNA (rRNA) sequences. This suggested that the diverse participants identified in each microecosystem belonged to a single species. To confirm species identity, we sampled the putative genetic diversity of multiple individuals of all morphotypes for each *Pristionchus* species in question. To do this, we sequenced the individual genomes of 49 specimens of *P. borbonicus*, and we sequenced rapidly evolving mitochondrial genes (*20*) for *P. sycomori* and *P. racemosae*. The genetic distance within each species was smaller than that between isolates of its selfing

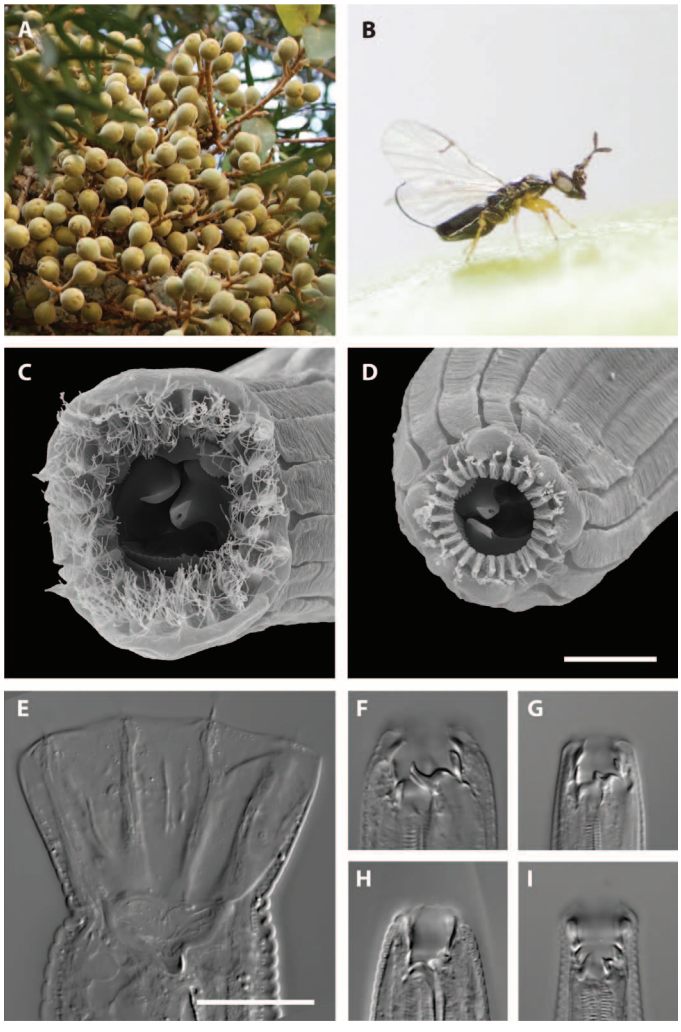

Fig. 1. Novelties and morphological diversity of nematode symbionts of figs. (**A**) Symbionts in the nematode genus *Pristionchus* are obligate associates of figs, such as *F. sycomorus* (shown here), in the African and Oriental tropics. (**B**) Fig-associated nematodes require transmission by pollinating wasps (*Ceratosolen* spp.), only a few of which are usually received by a given fig. (**C** and **D**) Two morphotypes (morphs I and II) of *P. borbonicus*, a symbiont of *F. mauritiana*. The beard-like labial morphology is a novelty known only for this species and *P. sycomori*. Scale bar, 10 μm. (**E** to **I**) Five alternative morphotypes of *P. racemosae*, a symbiont of the Australasian fig *F. racemosa*. Divergence of these morphs within species and with respect to the most closely related known fig associates is so great as to obscure homologies of traits or the morphs themselves. Scale bar, 20 μm.

congener *Pristionchus pacificus*: nucleotide diversity for *P. borbonicus* ($\pi = 0.0002$), in particular, was an order of magnitude lesser than for individual lineages of *P. pacificus* ($\pi = 0.002$) (*21*), and mitochondrial DNA (mtDNA) maximal sequence divergence between isolates of *P. sycomori* ($\hat{p} = 0.01$) and *P. racemosae* ($\hat{p} = 0.027$) was lesser than that for corresponding regions in *P. pacificus* ($\hat{p} = 0.054$ and $\hat{p} = 0.064$). To test whether genetic differences corresponded to any population structure among different morphotypes, we inferred a genotype network of more than 10,500 single-nucleotide polymorphic sites for individuals of *P. borbonicus* and mitochondrial haplotype networks for both *P. sycomori* and *P. racemosae*. No grouping of individuals by morphotype was observed, and different morphs instead had similar or identical haplotypes (Fig. 2, C to E). These results indicate the absence of reproductive isolation between different morphotypes within each species and that these morphotypes represent extreme intraspecific variation, possibly a polyphenism.

Condition dependence of diverse morphotypes

We next investigated the possibility that alternative morphotypes were the result of a polyphenism, specifically of condition-dependent induction. Examination of nematode populations in figs of *F. mauritiana* and *F. sycomorus* yielded four observations supporting polyphenism. First, surveys of nematodes by fig phase revealed differences in ratios of *Pristionchus* morphs between early and late interfloral figs. In figs that had recently received their pollinators, only a single minute, microbivorous morph of the associated *Pristionchus* species (morph V) emerged (Fig. 4A). Sequencing of individual nematodes present on the bodies of wasps that were captured exiting figs had confirmed that nematode species observed in figs, including *Pristionchus* spp., were transmitted as developmentally arrested (dauer) juveniles by the wasps (table S1). Therefore, morph V of *P. borbonicus* and *P. sycomori* represents postdispersal adults that are brought to young, receptive figs. Second, in generations of nematodes following this colonization event, morph V was never present, and instead, individuals of the four other morphs, including three types of putative carnivores (morphs I to III), were found (Fig. 4A and table S2). Third, observations of very late interfloral-phase figs revealed the occurrence of dauer larvae as progeny of morphs I to IV. After passage through the fig-wasp vector, these dauer larvae form phenotypes of morph V in early interfloral figs. Finally, we observed differences in ratios between sexes, suggesting that these morphs are induced from a single genotype in a sexually dimorphic manner (Fig. 4A), as described for the mouth polyphenism of other *Pristionchus* species (*22*).

To test whether different morphs were possible from the same nematode line, we developed a protocol to successfully rear one generation of fig-associated nematodes in laboratory culture. Indeed, we found that postdispersal adults (morph V) gave rise to an alternative nonpredatory morph of unknown function (morph IV) under laboratory conditions. Because nematodes could not be cultured further outside of the fig, environmental cues inducing the other morphs could not be identified. Taken together, surveys of nematode populations by fig phase and laboratory experiments indicate that the multiple morphs of fig-associated *Pristionchus* are the result of polyphenism and not genetic polymorphism.

Evidence for resource polyphenism

To test putative feeding specializations of individual morphs, we first inspected the behavior of nematode morphs in the laboratory. We found morphs I to III to be able to attack, kill, and feed on specimens of *Acrostichus* sp. and *Teratodiplogaster* sp., which frequently co-occur in the same figs (table S3). In addition, we screened the 49 genomes of individual specimens of *P. borbonicus* for the presence of non-*Pristionchus* nematode sequences. The presence of such sequences, presumably from the guts of sequenced individuals, would be an additional indicator of predatory behavior in the wild. Indeed, several individual genomes of morphs I and II showed an abundance of sequence reads for *Acrostichus* sp. and *Teratodiplogaster* sp., whereas such reads were not detected at high levels in morphs III to V (Fig. 4B). Thus, our metagenomic analysis distinguished morphs I and II as predators of other nematodes. A more detailed analysis of the feeding specializations of fig-associated *Pristionchus* awaits future studies of these minute animals in their tropical settings.

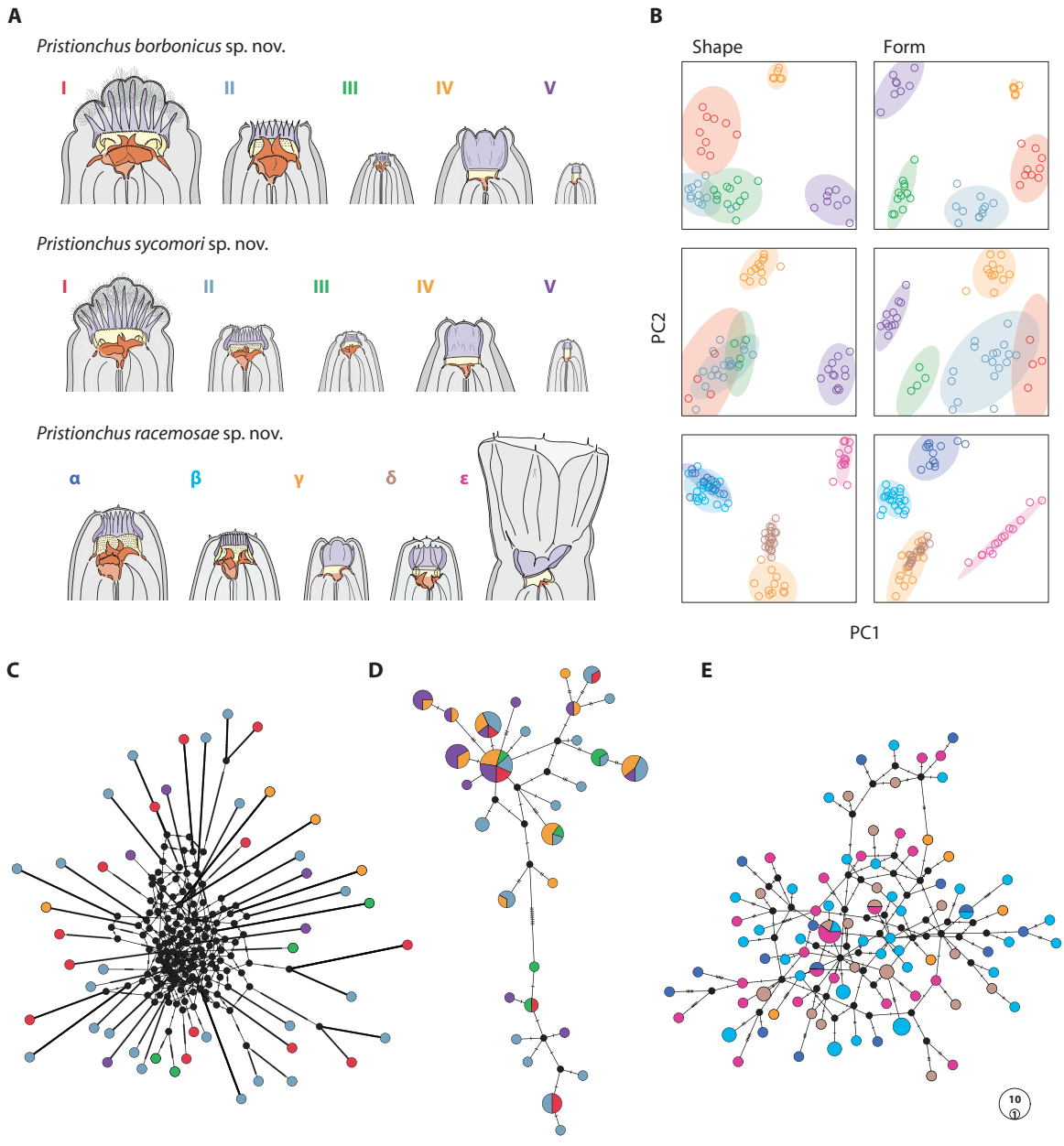

Fig. 2. Genetic and phenotypic diversity in fig-associated *Pristionchus* nematodes. (**A**) Discrete adult morphs of *P. borbonicus*, *P. sycomori*, and *P. racemosae*. Homologous mouthpart regions are color-coded across morphs and species. (**B**) Projections of the first two principal components of mouth shape and form (PC1, principal component 1; PC2, principal component 2). Colors indicate morphs, as coded by labels in (A). Ovals represent a 95% confidence interval of the mean. (**C**) Genotype network for 49 individuals of *P. borbonicus* based on 10,500 single-nucleotide polymorphic sites. (**D**) Haplotype network for 77 individuals of *P. sycomori* based on sequences of *ND1*, *Cytb*, and *COI* genes. (**E**) Haplotype network for 104 individuals of *P. racemosae* based on sequences of the *COI* gene. (C to E) Each circle represents a unique genotype or haplotype and is colored according to morphs, as coded by labels in (A); if greater than 1, pairwise differences between joined haplotypes are denoted by hatch marks and vertices, with the latter also showing theoretical intermediate nodes introduced by the algorithm; the size of circles is proportional to the number of individuals sharing the same haplotype.

Macroevolution via alternative phenotypes

Having uncovered a novel polyphenism of unprecedented complexity, we then explored the implications of such plasticity for macroevolution, or change following speciation events. Geometric morphometrics and PCA revealed that the addition of multiple morphs in fig-associated nematodes was accompanied by rapid divergence among morphs. Not only did some added morphs fall completely outside the range of phenotypes in other *Pristionchus* species, some morphs were irreconcilable with any of those of other species (for example, morphs I and V of *P. borbonicus* and *P. sycomori* and morph ε of *P. racemosae*) (Fig. 3A). Thus, diverging selection has occurred so rapidly that homologies of most morphs between African and Vietnamese lineages, which

are both associated with a relatively narrow clade of host trees/wasps (*23*), can no longer be determined in terms of either morphometrics or presence of qualitative structures (Figs. 1, 2A, 3A, and 5). Given the degree of disparity between morphs of dubious homology, it is possible that diverging selection among morphs has been supplemented by the loss and gain of new or recurring alternative morphotypes, resulting in intraspecific divergence within lineage diversification (Fig. 3B).

DISCUSSION

Multiplication of morphs and morphological diversification without speciation

Here, we have revealed an extreme case of morphological diversification without genetic divergence or isolation. This intraspecific disparity was observed particularly in adult mouthparts, which in a phylum of animals relatively limited in external morphology are widely regarded as the primary trait for determining their position in the food web (*24*). Even before a complete account of the natural history of this unusual system has been achieved, based on morphological, behavioral, and metagenomic evidence, we speculate that the diversity of feeding forms reflects large-scale ecological diversification. For example, the small microbivorous morph (V) of *P. borbonicus* and *P. sycomori* may develop fast to compete for an ephemeral bacterial food source, a common strategy in nematodes with simple, tube-like mouths (*25*). In contrast, predatory morphs emerge in the following generations, coincident with the proliferation of cohabiting wasp-transmitted nematodes in the fluid-filled cavities retained within the figs. In the examined African figs, other nematode species include plant parasites (*Schistonchus* spp. and *Bursaphelenchus* spp.), wasp parasites (*Parasitodiplogaster*

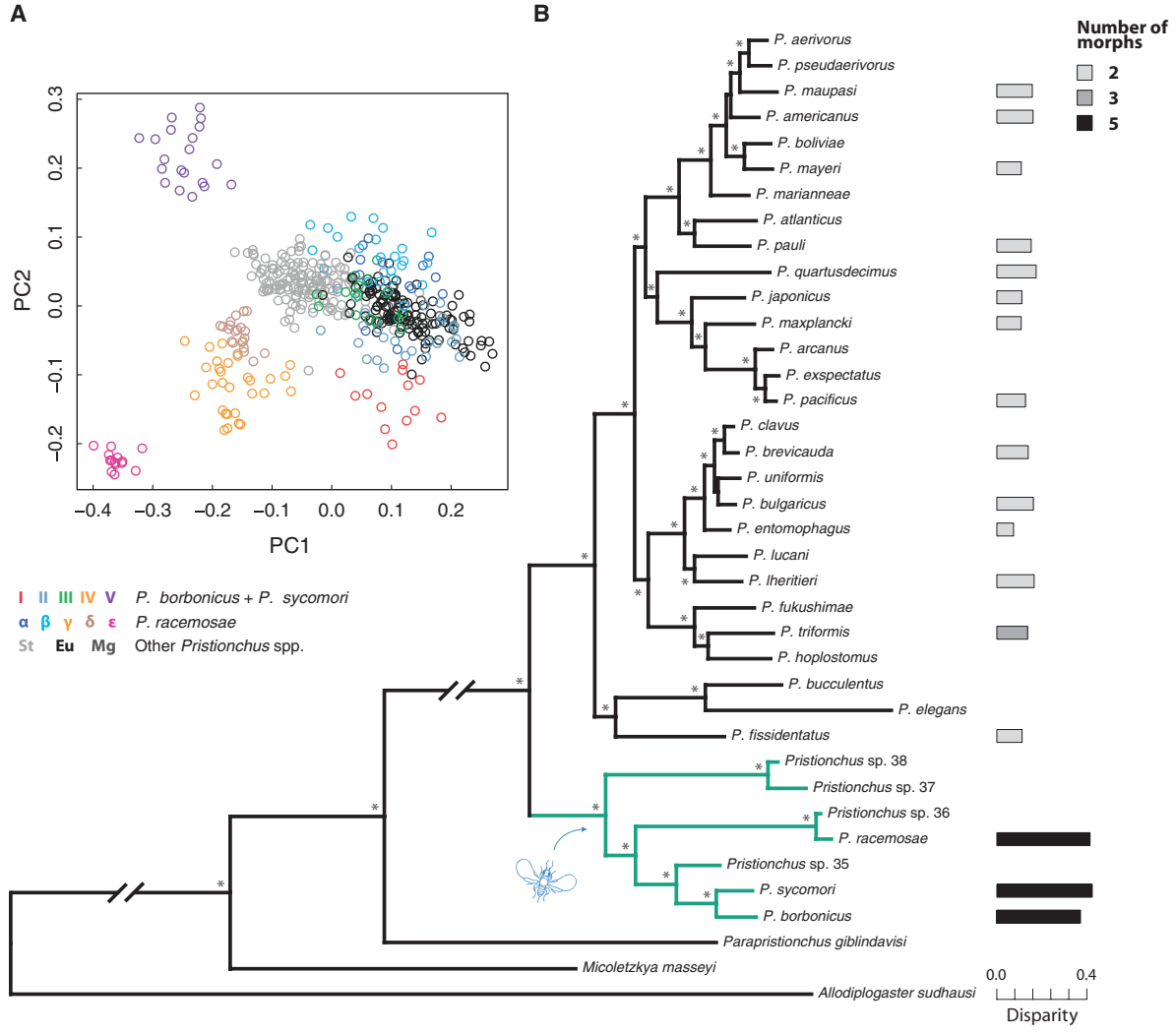

Fig. 3. Macroevolutionary disparity in fig symbionts relative to other *Pristionchus* species. (**A**) PCA of the mouth shape of 18 species of *Pristionchus* (PC1, principal component 1; PC2, principal component 2). Colors indicate morphs. (**B**) Phylogeny of *Pristionchus* spp. inferred from 18*S* and 28*S* rRNA genes and 27 ribosomal protein genes. Lineages that have radiated following a presumptively single fig colonization event are shown in green. Bars show disparity between morphs of selected polyphenic species, which was measured as maximal Euclidean pairwise distance in the morphospace between morph means. The color of bars is proportional to the number of morphs observed for a given fig-associated species. St, Eu, and Mg represent the two to three possible morphs in other *Pristionchus* species. Asterisk represents node support of 100% posterior probability.

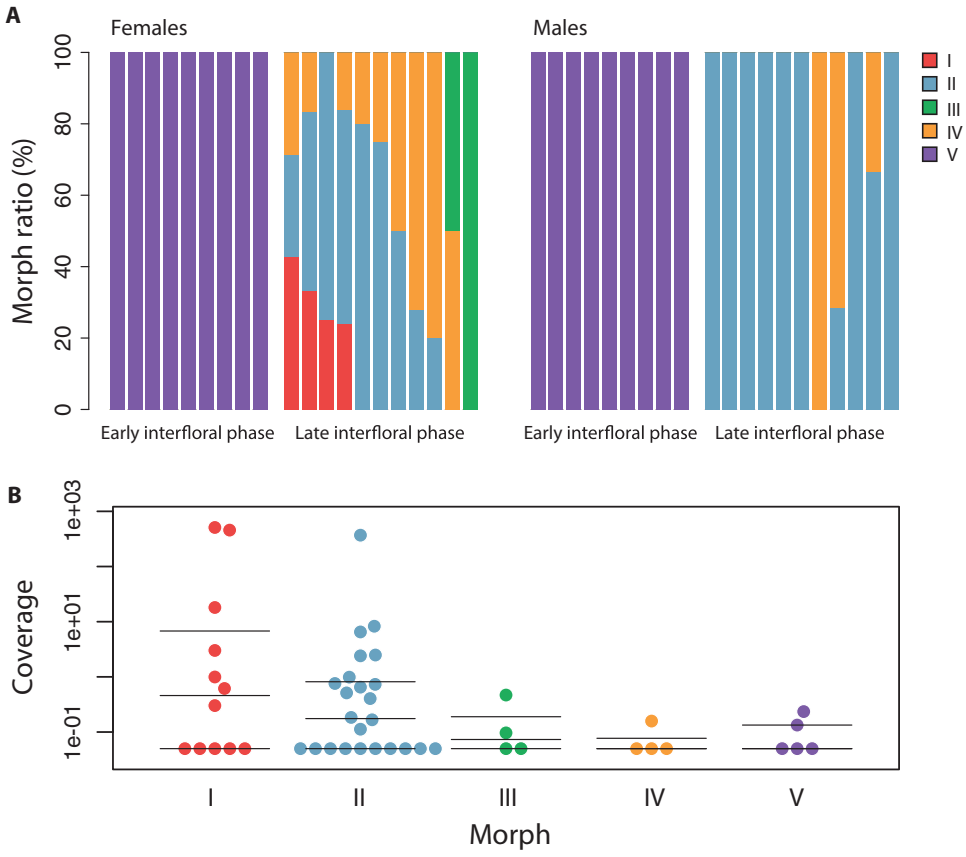

Fig. 4. Conditional dependence and sexual dimorphism of morph production in individual figs. (**A**) Individuals of *P. sycomori* in figs shortly after pollination are exclusively of the microbivorous morph in both males and females. In later stages of fig development, concomitant with the increase in complexity especially attributable to the presence and action of other wasp-transmitted nematode species, subsequent generations of *Pristionchus* nematodes give rise to alternative morphs, including both of predatory and of novel unknown function. Each bar represents the morph ratio in a single fig, with males and females for that fig represented in corresponding columns. Columns for late interfloral phase figs, which were not separated further by age, are ordered by composition only. (**B**) Predation in different morphs of *P. borbonicus*. Normalized coverage of 18*S* rRNA genes of non-*Pristionchus* nematodes detected in genomes of 49 individuals of *P. borbonicus* is shown. Thin lines mark 0.25, 0.5, and 0.75 quantiles.

spp.), omnivores (*Acrostichus* spp.), microbivores (*Caenorhabditis* spp.), and putative fungivores (*Teratodiplogaster* spp.) (table S3). Moreover, this intraspecific character displacement that has allowed niche partitioning within each nematode species is enabling *Pristionchus* nematodes to exploit the fig microecosystem in apparently novel, unknown ways, as indicated by at least one unprecedented form (morph ε) in the Vietnamese fig-associated *P. racemosae*. What makes this diversification remarkable is that the various morphotypes of all species were expressed at the same life stage, suggesting a hierarchy of developmental switches, in contrast to the ecological divergence that is typically limited to different developmental stages, as is common in zooplankton, holometabolous insects, and other nematodes.

Conditions for diversification without genetic isolation

The ability to produce any of five morphotypes at a single developmental stage, as evidenced by divergent feeding morphologies, is surprising in the absence of genetic isolation. The apparent uniqueness of this system therefore demands some explanation. First, a significant (albeit not exclusive) feature of *Pristionchus* fig symbionts is the ancestral presence of a feeding dimorphism (*17*) and its associated developmental switch (*22*), which may have disposed alternative morphs to relaxed selection on conditionally expressed phenotypes (*26*, *27*). Indeed, the macroevolutionary maintenance of this dimorphism apparently led to increased rates of morphological evolution in this nematode family (*17*) and thus may also have facilitated the genetic variation needed to add successive switches to the mouth polyphenism. Alternatively, an ancestral polyphenism may have facilitated the recurrence of forms, allowing the rapid re-establishment of morphotypes (*6*) to result in a multiplied polyphenism. For example, morphs α and β of *P. racemosae* show characters (that is, stomatal rugae) that are absent from all other *Pristionchus* and its closest outgroups but are present in distant lineages of Diplogastridae (*17*), indicating the possibility of recurrence, if not uncanny convergent evolution. A second distinguishing feature is the bottlenecked vertical transmission of nematodes by their insect vectors. This mode of transmission presumably precludes the reliable transmission of multiple genetically distinct morphs to new figs, which may have promoted the maintenance of polyphenism over genetic assimilation of alternative phenotypes. Third, the small physical dimensions and spatially overlapping niches within figs may simply preclude genetic isolation in sympatry. In principle, character displacement between "allopatric" species (that is, species coevolved with fig and wasp

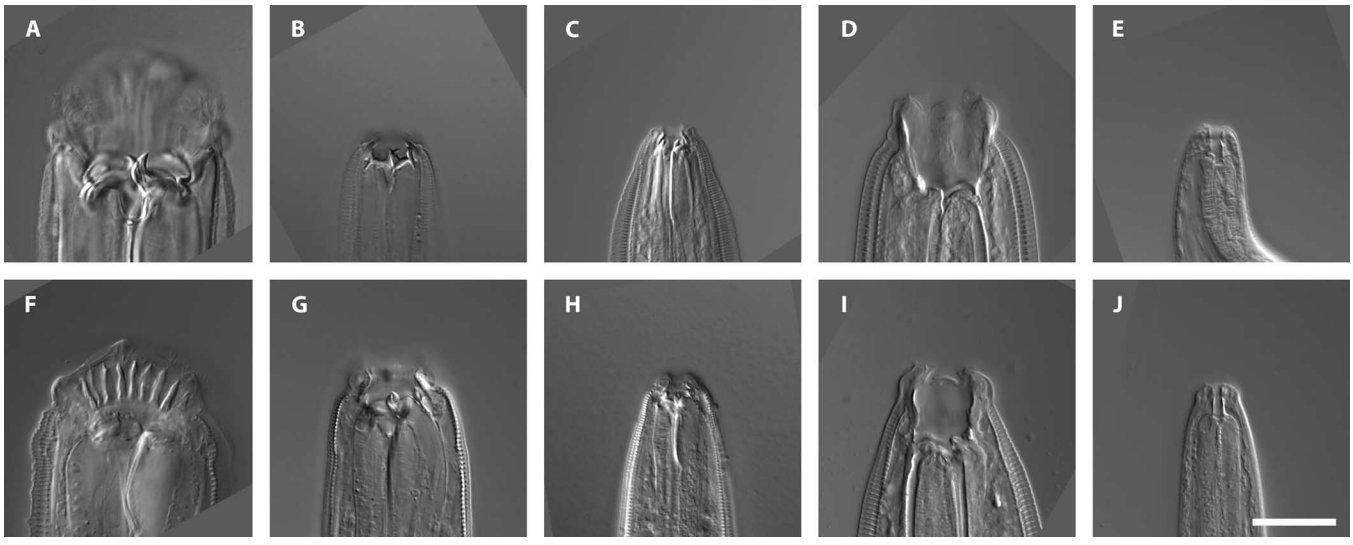

Fig. 5. Discrete morphs present in *P. borbonicus* (A to E) and *P. sycomori* (F to J). For both species, morphs are (from left to right) as follows: I, II, III, IV, and V. Scale bar, 20 μm.

hosts) with multiple phenotypes, which in this case would result from host switching by the wasp vector, could ultimately lead to the genetic assimilation of alternative forms in competing species (*28*). However, the repeated occurrence of five morphs suggests that any possible competition between otherwise allopatric species is not prevalent enough in this system to have led to the assimilation of alternative morphotypes in different species.

Conclusions

In summary, given the "empty niche" conditions predisposing an ecosystem to the trophic diversification of its colonists (in particular, low ecological complexity, previously limited immigration of species, and underutilized resources) (*2*), a pre-existing polyphenism, and vertically transmitted founder populations could have together facilitated macroevolutionary-scale diversification in fig-associated nematodes without lineage splitting. Despite the idiosyncrasies of the fig microecosystem, our findings support the prediction that "stem plasticity" in a lineage allows diversifying selection into multiple ecological roles (*6*, *29*). Thus, our findings reveal an alternative possibility to the principle that substantial phenotypic evolution only follows periods of speciation (*1*, *30*) and that developmental plasticity can lead to the multiplication of discontinuous novelties from a single genotype.

Taxonomy

P. borbonicus Susoy, Kanzaki, Herrmann, Ragsdale, and Sommer sp. nov. (Phylum Nematoda Potts, 1932; Order Rhabditida Chitwood, 1933; Family Diplogastridae Kreis, 1932).

Etymology. The species epithet is the Latin adjectival demonym for Île Bourbon, the former name for the island of the type locality of this species.

Holotype. Adult female of morph I is deposited in the University of California Riverside Nematode Collection (UCRNC).

Paratypes. Ten paratypes are deposited in the UCRNC, whereas 10 paratypes are deposited in the Swedish Museum of Natural History (Stockholm, Sweden).

Locality. Type specimens were collected at Grand Étang, La Réunion Island.

Type host and vector. Type specimens were isolated from within sycones of *F. mauritiana* Lamarck, 1788 (Moraceae), in association with *C. coecus* Coquerel, 1855 (Hymenoptera: Agaonidae).

Description. Body habitus, pharynx, female reproductive tract, male testis, and positions of ventral body openings are typical of *Pristionchus* nematodes (Fig. 1, C and D, Fig. 2A, and Fig. 5, A to E). Cuticle with fine annulation and thick, offset longitudinal alae are found on the entire body diameter, extending from the labial region to the tail, except for morph V, in which ridges are indistinct. Adults consist of five morphs. Because these morphs are of uncertain homology with respect to the eurystomatous and stenostomatous morphs of other *Pristionchus* species, we adopt a neutral nomenclature (that is, morphs I to V) for the new species:

Morph I: Body larger than those of other morphs, head widening just anterior to the labial region; lips large, lateral lips higher and wider than subventral and subdorsal lips; labial region with conspicuous "beard" (a circumstomatal ring of thin cuticular filaments originating from anterior cheilostom); pre-gymnostomatal cheilostom twice as high as gymnostom, with anteriorly tapering rugae separated from each other for most of their length; gymnostom thick, barrel-shaped, overlapping cheilostom for most of height, finely serrated at anterior margin; pro-mesostegostom projecting into one dorsal and two subventral anteriorly serrated lobes; metastegostom with claw-like dorsal tooth, claw-like right subventral tooth, and large, coarsely serrated left subventral ridge extending dorsally past most of the dorsal tooth; postdental region (telostegostom) deeper ventrally than dorsally, sclerotized.

Morph II: Head narrowing just anterior to the labial region; with six offset lips, lateral lips smaller than subventral and subdorsal lips; pre-gymnostomatal cheilostom same height as gymnostom, with closely spaced, tapering rugae, each tipped with several filaments and extending past the stomatal opening; gymnostom with thick walls, overlapping cheilostom for most of height, with heavy punctation and fine anterior serration; pro-mesostegostom with small projecting, serrated lobes; meta- and telostegostom as in morph I.

Morph III: Head tapered, with small but distinct lips; stoma small; cheilostom with sharp anterior taper, with minute, tightly packed rugae not extending past the stomatal opening; gymnostom thin, barrel-shaped,

overlapping cheilostom for most of height, with fine punctation; small projecting lobes in mesostegostom indistinct or absent; metastegostom with small dorsal and right subventral claw-like teeth and left subventral plate with two or three denticles, telostegostom as in morph I.

Morph IV: With six offset, separate, and thin-walled bulging lips, subdorsal and subventral lips larger than lateral lips, with pointed labial papillae; cheilostom large, vacuous, undivided; gymnostom thin, smooth, narrower than and barely overlapping cheilostom; stegostom simple, smooth, except for a small dorsal bulge with thickened cuticle; telostegostom narrow, sclerotized.

Morph V: Body thin, smaller than other morphs, sometimes less than a third of the size of other morphs (that is, I and IV); stoma tube-like; cheilostom undivided, toroid-shaped; gymnostom slightly taller than cheilostom, barely overlapping the latter, anteriorly tapered; stegostom simple, smooth, except for a small dorsal bulge with thickened cuticle.

Eight pairs of genital papillae are arranged as <v1, v2, (C, v4), ad, (pd, Ph, v5 to v7)>, such that v3d is absent, v1 and v4 are each separated from v2 by ca. one anal body width, ad is equidistant between v4 and v5 to v7, and pd is clearly anterior to v5. Spicules have large manubrium, twisted lamina, and calomus anteriorly, with raised ventral ridge. Tail is filiform and long in males and females (ca. seven to nine cloacal/anal body widths) of morphs I to IV; tails of both sexes are short and conical in morph V.

Diagnosis. The new species is distinguished from all other Diplogastridae, except for *P. sycomori* sp. nov. and *P. racemosae* sp. nov., by the presence of five morphs and by having morphs of laterally symmetrical and laterally asymmetrical stomatal structures in the same species. It is distinguished from all species, except for *P. sycomori* sp. nov., by the presence of a form (morph I) with a "bearded" inner stomatal opening, the lateral sides of which are axially longer than the dorsal and ventral margins. The new species is distinguished from *P. sycomori* sp. nov. by morph V having a thin versus posteriorly widened cheilostomatal toroid and by its unique 18*S* rRNA barcode (ca. 850-bp fragment defined by primers SSU18A and SSU26R; GenBank accession number KT188856), which differs from that of *P. sycomori* sp. nov. by 15 unique sites.

P. sycomori Susoy, Kanzaki, Kruger, Ragsdale, and Sommer sp. nov.

Etymology. The species epithet is the Latin genitive for that of its fig host, *F. sycomorus*.

Holotype. Adult female of morph I is deposited in the UCRNC.

Paratypes. Ten paratypes are deposited in the UCRNC, whereas 10 paratypes are deposited in the Swedish Museum of Natural History (Stockholm, Sweden).

Locality. Type specimens were collected from the Manie van der Schijff Botanical Garden at the University of Pretoria (Pretoria, South Africa).

Type host and vector. Type specimens were isolated from within sycones of the sycamore fig *F. sycomorus* Linneaus, 1753 (Moraceae), in association with *C. arabicus* Mayr, 1906 (Hymenoptera: Agaonidae).

Description. Body habitus, pharynx, female reproductive tract, male testis, and positions of ventral body openings are typical of *Pristionchus* nematodes (Fig. 2A and Fig. 5, F to J). Cuticle with fine annulation and thick, offset longitudinal alae are found on the entire body diameter, extending from the labial region to the tail, except for morph V, in which ridges are indistinct. Adults consist of five morphs. The nomenclature of morphs follows that used for *P. borbonicus* sp. nov. (that is, I to V), with which homologies of morphs could be assigned:

Morph I: Body larger than those of other morphs, head not tapering anterior to the labial region; lips large, lateral lips higher and wider than subventral and subdorsal lips; labial region with conspicuous beard (a circumstomatal ring of thin cuticular filaments originating from anterior cheilostom); pre-gymnostomatal cheilostom twice as high as gymnostom, with anteriorly tapering rugae separated from each other for most of their length; gymnostom thick, barrel-shaped, overlapping cheilostom for most of height, finely serrated at anterior margin; pro-mesostegostom projecting into one dorsal and two subventral anteriorly serrated lobes; metastegostom with claw-like dorsal tooth, claw-like right subventral tooth, and coarsely serrated left subventral ridge slightly overlapping the dorsal tooth; telostegostom deeper ventrally than dorsally, sclerotized.

Morph II: Head narrowing just anterior to the labial region; with six offset lips, lateral lips smaller than subventral lips; pre-gymnostomatal cheilostom with same height as gymnostom, with closely spaced, tapering rugae, each tipped with several filaments and extending past the stomatal opening; gymnostom thick, overlapping cheilostom for most of height, with fine anterior serration and with heavy punctation on medial surface; pro-mesostegostom with small projecting lobes; meta- and telostegostom as in morph I.

Morph III: Head tapered, with clearly offset, squared lips; stoma small; cheilostom with sharp anterior taper, with minute, tightly packed rugae not extending past the stomatal opening; gymnostom thin, barrel-shaped, overlapping cheilostom for most of height, with fine punctation; small projecting lobes in pro-mesostegostom indistinct or absent; metastegostom with small dorsal and right subventral claw-like teeth and left subventral plate with two to three denticles; telostegostom as in morph I.

Morph IV: With six offset, separate, thick-walled bulging lips, subdorsal and subventral lips larger than lateral lips, with pointed labial papillae; cheilostom large, vacuous, undivided; gymnostom thin, smooth, narrower than and barely overlapping cheilostom; stegostom simple, smooth, except for a small dorsal bulge with thickened cuticle; telostegostom narrow, sclerotized.

Morph V: Body thin, smaller than other morphs, sometimes less than a third of the size of other morphs (that is, I and IV); stoma tube-like; cheilostom undivided, and distinctly wider posteriorly, such that wall is triangular in section; gymnostom clearly taller than cheilostom, barely overlapping the latter, anteriorly tapered; stegostom simple, smooth, except for a small dorsal bulge with thickened cuticle.

Tail is filiform and long in males and females (ca. seven to nine cloacal/anal body widths) of morphs I to IV; tails of both sexes are short and conical in morph V.

Diagnosis. The new species is distinguished from all other Diplogastridae, except for *P. borbonicus* sp. nov. and *P. racemosae* sp. nov. (see below), by the presence of five morphs and by having morphs of laterally symmetrical and laterally asymmetrical stomatal structures in the same species. It is distinguished from all species, except *P. borbonicus* sp. nov., by the presence of a form (morph I) with a bearded inner stomatal opening, the lateral sides of which are axially longer than the dorsal and ventral margins. The new species is distinguished from *P. borbonicus* sp. nov. as described above, including its unique 18*S* rRNA barcode (ca. 850-bp fragment defined by primers SSU18A and SSU26R; GenBank accession number KT188857).

***P. racemosae* Susoy, Kanzaki, Nguyen, Ragsdale, and Sommer sp. nov.**

Etymology. The species epithet is the Latin genitive for that of its fig host, *F. racemosa*.

Holotype. Adult female of morph ε is deposited in the UCRNC.

Paratypes. Ten paratypes are deposited in the UCRNC, whereas 10 paratypes are deposited in the Swedish Museum of Natural History (Stockholm, Sweden).

Locality. Type specimens were collected from the campus of the Institute of Ecological and Biological Sciences, Vietnamese Academy of Science and Technology (Cau Giay, Hanoi, Vietnam).

Type host and vector. Type specimens were isolated from within sycones of the cluster fig *F. racemosa* Linneaus, 1753 (Moraceae), in association with *C. fusciceps* Mayr, 1885 (Hymenoptera: Agaonidae).

Description. Body habitus, pharynx, female gonad, male testis, and positions of ventral body openings are typical of *Pristionchus* nematodes, except for morph-specific characters as specified below (Fig. 1, E to I, and 2A). Adults consist of five morphs. Because homologies of morphs are uncertain with respect to the morphs of other *Pristionchus* species or with the five morphs of *P. borbonicus* sp. nov. and *P. sycomori* sp. nov., an independent nomenclature (that is, α to ε) is used here. Cuticle of morphs α to δ has annulation, as well as rings of punctations that form evenly spaced longitudinal striations; cuticle of morph ε is thick, with large annulations and no apparent punctation or longitudinal striation. Pharynx of morphs α to δ has a "fish-bone" or zipper-like lumen; pharyngeal lumen of morph ε is smooth. Adults consist of five adult morphs:

Morph α: Head wide, not tapering posterior to the labial region; with six similarly sized, rounded, slightly offset lips; pre-gymnostomatal cheilostom slightly taller than gymnostom, with tightly packed rugae originating from the anterior to posterior base of cheilostom; gymnostom with heavy punctations, anterior margin consisting of six "wave"-like projections radially offset from lips by 30°; pro-mesostegostom without apparent projecting lobes; metastegostom with claw-like dorsal tooth, claw-like right subventral tooth, and coarsely serrated left subventral ridge slightly overlapping the dorsal tooth; telostegostom deeper ventrally than dorsally, deeper than wide, sclerotized.

Morph β: Head narrow; lips indistinct; pre-gymnostomatal cheilostom shorter than gymnostom, with tightly packed rugae originating from the posterior base of cheilostom; gymnostom with fine punctation, anterior margin slightly wavy but without distinct projections; metastegostom with claw-like dorsal tooth, claw-like right subventral tooth, and coarsely serrated left subventral ridge not overlapping the dorsal tooth; telostegostom as in morph α.

Morph γ: Cheilostom vacuous, undivided; gymnostom thin, smooth, narrower than and barely overlapping cheilostom; stegostom simple, smooth, except for a small dorsal bulge with thickened cuticle.

Morph δ: Six lips of similar size, distinct only at the stomatal opening; cuticle thick distally and vacuolated medially (internally), separated into adradial bulges, the anterior margins of which form a ring of sharp anterior points; gymnostom short, barely overlapping cheilostom, narrower than cheilostom, distally thickened and medially vacuolated; metastegostom with a small, thin, triangular dorsal tooth and with two symmetrical, subventral, dagger-like teeth larger than the dorsal tooth; telostegostom shallow, weakly sclerotized.

Morph ε: Large morph of variable body size, often twice the length of other morphs; labial region expanded into a large (longer than one labial body width), umbrella-like flap, the left side of which is open as a slit with a round opening at the base, and with six ribs consisting of labial papillae within cuticle; amphids present as small pores near the tip of the umbrella-like structure; cheilostom smooth, anterior margin marked by per- and interradial notches; cheilostom and gymnostom dorsoventrally isometric, such that the ventral boundary between these regions projects inwardly like a tooth; gymnostom smooth; stegostom simple, smooth, except for a flat, triangular thickening of cuticle in place of the dorsal tooth; telostegostom not sclerotized, indistinct.

Nine pairs of male genital papillae are arranged as <v1, (v2d, v3), C, v4, (ad, Ph), (v5 to v7), pd>, such that v3 is closer to (⅓ of a cloacal body width anterior to) v1 than to v4, and v2d and v3 are at the same level. Manubrium is wide and longitudinally flat, with a ventral hook projecting posteriad behind the rest of the spicule; posterior part of the spicule has a distinct dorsal keel that is as deep as the spicule itself; gubernaculum is flared anteriorly, such that ventral and dorsal walls separate at an angle of 45°. Vagina is expanded into an axially "heart-shaped" recaptaculum seminis. Tails of both sexes are conical (ca. four to five cloacal/anal body widths).

Diagnosis. The new species is distinguished from all other Diplogastridae, except for *P. borbonicus* sp. nov. and *P. sycomori* sp. nov. by the presence of five morphs and by having morphs of laterally symmetrical and laterally asymmetrical stomatal structures in the same species. The new species is diagnosed from the latter two species by the presence of a form (morph δ) with a vacuolated cheilostom separated into adradial divisions and by the presence of a form (morph ε) with an umbrella-like labial flap that is open on the left side and that extends more than a labial body diameter anterior from the stomatal opening. It is further distinguished from all other nematode species by its unique 18*S* rRNA barcode (ca. 850-bp fragment defined by primers SSU18A and SSU26R; GenBank accession number KT188859).

MATERIALS AND METHODS

Nematode isolation

To sample nematodes, we collected figs from *F. mauritiana* (La Réunion), *F. sycomorus* (South Africa), and *F. racemosa* (Vietnam). Individual figs were dissected, and all nematodes that were present in the cavity of the fig were collected. Nematodes that were identified as *Pristionchus* were individually transferred into a sterile buffer, which was developed to allow short-term culture of fig-associated nematodes. The composition of the buffer approximated the fig environment and was based on the chemical composition of raw figs (*31*). We then screened *Pristionchus* nematodes for their mouth phenotypes using a light microscope or stereomicroscope before proceeding with further experiments.

Genome sequencing of individuals of *P. borbonicus*

We isolated adult individuals of *P. borbonicus* from freshly collected figs of *F. mauritiana*. Living nematode individuals were kept in a sterile buffer for 10 to 15 min to minimize possible surface contamination, after which the nematodes were individually transferred into a lysis solution and thereafter frozen until DNA extraction. The DNA of individual nematodes was isolated using the MasterPure DNA Purification Kit (Epicentre), following the manufacturer's protocol for DNA purification from tissue samples. The DNA was sheared using a S220 focused ultrasonicator (Covaris) under the following operation conditions: 10 dc, 4 i, 200 cpb, and 80 s. Genomic paired-end libraries were prepared using Low Input Library Preparation Kit (Clontech Laboratories). Size selection was performed on final libraries using BluePippin and 1.5%

agarose gel cassettes (Sage Science). Paired-end libraries were sequenced using a HiSeq 2000 system (Illumina). mRNA libraries that were used for scaffolding (see below) were prepared from TRIzol-lysed individuals. Total RNA was isolated from single specimens using the PureLink RNA micro kit (Invitrogen), after which complementary DNA (cDNA) was prepared using the SMARTer Ultra Low Input cDNA synthesis kit (Clontech Laboratories). cDNA was sheared using the following operation conditions: 10 dc, 4 i, 200 cpb, 40 s. Paired-end libraries were prepared and sequenced as described above.

Genome assembly and analysis of the molecular diversity of *P. borbonicus*

A draft genome assembly for *P. borbonicus* was generated from the DNA-sequencing data of a single individual using the SOAPdenovo assembler (*32*). Genomic and transcriptomic data from other individuals were used for additional scaffolding and gap closing (*33*, *34*). After discarding contamination [contigs with more than half of the sequence showing a >95% identity to non-Diplogastrid sequences in the National Center for Biotechnology Information (NCBI) nucleotide database], the final assembly comprised 157,322 contigs spanning 155 Mb with an N50 contig size of 9.4 kb. Genomic data for 49 individuals were aligned to the *P. borbonicus* draft genome using a Burrows-Wheeler aligner (*35*). Single-nucleotide polymorphism (SNP) calling and diversity analysis were performed as previously described (*21*). Variable sites with coverage in all samples were extracted to reconstruct a TCS genotype network (that is, a phylogenetic network estimation using statistical parsimony) (*36*) using PopART 1.7 (http://popart.otago.ac.nz).

Haplotype diversity of *P. sycomori* and *P. racemosae*

We extracted DNA from living or DESS (a solution containing dimethyl sulfoxide, disodium EDTA, and saturated NaCl)–preserved individuals. Fragments of *ND1*, *Cytb*, and *COI* mitochondrial genes were amplified and sequenced for *P. sycomori*, and sequences of the *COI* gene were obtained for individuals of *P. racemosae*. The sequences were quality-checked and assembled using Geneious 6.1.4 and aligned using Muscle 3.8 (*37*). The concatenated alignment of *ND1*, *Cytb*, and *COI* genes for 77 individuals of *P. sycomori* contained 52 variable and 36 parsimony-informative sites. The alignment of the *COI* sequences of 104 individuals of *P. racemosae* had 98 variable and 54 parsimony-informative sites. Maximal mtDNA sequence divergence between isolates of the same species was estimated by *p* distance using MEGA 6 (*38*). For comparison, we estimated sequence divergence in corresponding regions of the mtDNA of 104 *P. pacificus* strains (*21*). TCS haplotype networks were inferred from those alignments using PopART 1.7.

Geometric morphometrics and analysis of disparity

To quantify the mouth morphology of different morphs and species of *Pristionchus*, we used a geometric morphometrics approach adapted from a previous study (*17*). Briefly, 13 two-dimensional landmarks were assigned to homologous structures of the nematode stoma (mouth), as informed by fine structural anatomy (*39*, *40*). In addition to 11 landmarks used previously (*17*), two landmarks that marked the position of dorsal and ventral labial sensilla were recorded (fig. S1). Landmark coordinates were identified twice for each specimen, digitalized using tpsDig2 (*41*), and averaged for each specimen using MorphoJ (*42*). In total, our data set included 18 species and 450 individuals of *Pristionchus*. PCA of shape was performed on Procrustes-superimposed landmark coordinates, and PCA of stomatal form was performed on superimposed landmark coordinates + logarithm-transformed centroid size (*18*, *19*). The proportion of total variance explained by the first three principal component axes for all analyses is given in table S4. Disparity between different morphs of polyphenic species of *Pristionchus* was calculated as the maximal Euclidean pairwise distance between morph means in Procrustes shape space using the MATLAB package MDA (*43*). Principal components that explained more than 10% of the total variance were included in the analysis.

Testing mode of transmission of nematodes

To confirm that *Pristionchus* nematodes were transmitted by wasps pollinating the figs, we brought ripe figs of *F. mauritiana* into the laboratory. The figs were kept at room temperature until a new generation of pollinator wasps (*C. coecus*) emerged from them. Emerging female wasps were collected in a trap and then preserved at −25°C until further examination. Ten wasps were placed in 2 ml of water with 0.1% Triton X and kept on a shaker for 1 hour to allow dispersal (dauer) juvenile nematodes to detach from the body surface of the wasp. Eighty-four nematode dauers were collected, and the DNA from individual dauers was extracted. We then amplified and sequenced a portion of the 18*S* rRNA gene, specifically an 830-bp diagnostic fragment developed for nematode identification (*44*, *45*). The sequences were compared to those of nematodes previously isolated from figs of *F. mauritiana*.

Induction of alternative phenotypes

We collected figs of *F. sycomorus* of early interfloral phase and confirmed that only males and females of morph V of *P. sycomori* were present. We then collected 20 gravid females from different figs, transferred them into a 3-cm Petri dish filled with the buffer described above, and provided them with a microbial food supply that enabled their reproduction on plates (that is, mixed bacteria extracted from host figs, 1 mg of *Escherichia coli* strain OP50, or 1 mg of *Erwinia typographi* strain P11-1, all of which resulted in the same induced phenotype). The females were allowed to lay eggs, which in 8 days developed into adult males and females. The mouth phenotypes of the offspring were then scored.

Metagenomic analysis of predation

Genomic data of 49 individuals of *P. borbonicus* were screened for 18*S* rRNA sequences using PhyloSift 1.0.1 (*46*). Paired reads that had similarity to eukaryotic 18*S* rRNA reference genes were extracted and assembled using Geneious 6.1.4. Resulting contigs were searched against the NCBI database using BLAST, and contigs that matched nematode 18*S* rRNA genes were identified. Those nematode 18*S* rRNA genes were used as references to which genomic reads of individual *P. borbonicus* nematodes were mapped, and the normalized coverage for non-*Pristionchus* nematode and *Pristionchus* 18*S* rRNA was estimated. Normalized coverage was calculated as follows: (coverage of non-*Pristionchus* 18*S* rRNA/coverage of *Pristionchus* 18*S* rRNA) × 3000, where 3000 is the average coverage of the 18*S* rRNA gene for *P. borbonicus* individuals.

Phylogeny of *Pristionchus*

We inferred the phylogeny of 28 described and 7 new species of *Pristionchus*. In addition to the three species described herein, we included species isolated from four other species or populations of *Ficus* (*Sycomorus*), section *Sycomorus* [*Ficus sur* in South Africa (*Pristionchus* sp. 35), *F. racemosa* in Australia (*Pristionchus* sp. 36), and *Ficus variegata* in

Australia (*Pristionchus* sp. 37) and Okinawa, Japan (*Pristionchus* sp. 38)] in our phylogenetic analysis to test the monophyly of fig-associated *Pristionchus*. The diplogastrid nematodes *Parapristionchus giblindavisi*, *Micoletzkya masseyi*, and *Allodiplogaster sudhausi* were included as outgroups (*17*). The phylogeny was inferred from a concatenated alignment of 27 ribosomal protein genes and 18*S* and 28*S* rRNA genes. The ribosomal protein genes included in the analysis were *rpl-1*, *rpl-2*, *rpl-10*, *rpl-14*, *rpl-16*, *rpl-23*, *rpl-26*, *rpl-27*, *rpl-27a*, *rpl-28*, *rpl-29*, *rpl-30*, *rpl-31*, *rpl-32*, *rpl-34*, *rpl-35*, *rpl-38*, *rpl-39*, *rps-1*, *rps-8*, *rps-14*, *rps-20*, *rps-21*, *rps-24*, *rps-25*, *rps-27*, and *rps-28*, with conditions as described previously (*47*). Ribosomal protein gene sequences were individually aligned by predicted translation using default settings in Muscle 3.8, and rRNA genes were aligned using the G-INS-I algorithm and default settings in MAFFT 7.1 (*48*). The final alignment included 15,902 total and 3485 parsimony-informative sites. The fraction of missing data was less than 16%.

The phylogeny was inferred under the Bayesian optimality criterion, as implemented in MrBayes 3.2.2 (*49*). The inference was performed on the CIPRES Science Gateway (*50*). For the analyses, the data set was partitioned into three subsets: two for 18*S* and 28*S* rRNA genes, which were analyzed using a "mixed" + Γ model, and the third for the ribosomal protein genes, which was analyzed under a codon + Γ model. Model parameters were unlinked across partitions. Two independent analyses, each containing four chains, were run for 20 million generations, with chains sampled every 1000 generations. After confirming convergence of runs and mixing of chains using Tracer 1.6 (*51*), the first half of generations was discarded as burn-in, and the remaining tree topologies were summarized to generate a 50% majority-rule consensus tree.

Composition of buffer for short-term maintenance of fig nematodes

The buffer was composed of the following: potassium chloride, 55 mM; dipotassium phosphate, 3.6 mM; calcium chloride dihydrate, 8.7 mM; magnesium sulfate, 6.65 mM; ascorbic acid, 57 μM; sorbitol, 1.1 mM; ribitol, 1.3 mM; mannitol, 1.1 mM; citric acid, 0.5 mM; mallic acid, 0.75 mM; BME Vitamin Solution (100×) B 6891 (Sigma-Aldrich), 10 ml/liter; trace metals solution (1.86 g of disodium EDTA, 0.69 g of $FeSO_4{\cdot}7H_2O$, 0.2 g of $MnCl_2{\cdot}4H_2O$, 0.29 g of $ZnSO_4{\cdot}7H_2O$, and 0.025 g of $CuSO_4{\cdot}5H_2O$, in 1 liter of H_2O), 10 ml/liter. The pH of the buffer was adjusted to 7.5 with potassium hydroxide, and the buffer was sterilized by filtering (Nalgene 295-4545).

SUPPLEMENTARY MATERIALS

Supplementary material for this article is available at http://advances.sciencemag.org/cgi/content/full/2/1/e1501031/DC1

Fig. S1. Positions of 13 two-dimensional landmarks recorded for the stoma of fig-associated *Pristionchus* species.

Table S1. Nematode dauers transmitted by wasps (*C. coecus*) emerging from ripe figs of *F. mauritiana*.

Table S2. Ratio of morphs in a single fig sycone for males and females of *P. sycomori*.

Table S3. Nematode species isolated from sycones of *F. mauritiana*, *F. sycomorus*, and *F. racemosa*.

Table S4. Proportion of variance explained by the first three principal component axes in the PCA of mouth form and shape for fig-associated *Pristionchus* species.

REFERENCES AND NOTES

1. G. G. Simpson, *The Major Features of Evolution* (Columbia Univ. Press, New York, 1953), 434 pp.
2. D. Schluter, *The Ecology of Adaptive Radiations* (Oxford Univ. Press, Oxford, 2000), 288 pp.
3. S. Gavrilets, J. B. Losos, Adaptive radiation: Contrasting theory with data. *Science* **323**, 732–737 (2009).
4. D. Brawand, C. E. Wagner, Y. I. Li, M. Malinsky, I. Keller, S. Fan, O. Simakov, A. Y. Ng, Z. W. Lim, E. Bezault, J. Turner-Maier, J. Johnson, R. Alcazar, H. J. Noh, P. Russell, B. Aken, J. Alföldi, C. Amemiya, N. Azzouzi, J.-F. Baroiller, F. Barloy-Hubler, A. Berlin, R. Bloomquist, K. L. Carleton, M. A. Conte, H. D'Cotta, O. Eshel, L. Gaffney, F. Galibert, H. F. Gante, S. Gnerre, L. Greuter, R. Guyon, N. S. Haddad, W. Haerty, R. M. Harris, H. A. Hofmann, T. Hourlier, G. Hulata, D. B. Jaffe, M. Lara, A. P. Lee, I. MacCallum, S. Mwaiko, M. Nikaido, H. Nishihara, C. Ozouf-Costaz, D. J. Penman, D. Przybylski, M. Rakotomanga, S. C. P. Renn, F. J. Ribeiro, M. Ron, W. Salzburger, L. Sanchez-Pulido, M. E. Santos, S. Searle, T. Sharpe, R. Swofford, F. J. Tan, L. Williams, S. Young, S. Yin, N. Okada, T. D. Kocher, E. A. Miska, E. S. Lander, B. Venkatesh, R. D. Fernald, A. Meyer, C. P. Ponting, J. T. Streelman, K. Lindblad-Toh, O. Seehausen, F. Di Palma, The genomic substrate for adaptive radiation in African cichlid fish. *Nature* **513**, 375–381 (2014).
5. S. Lamichhaney, J. Berglund, M. S. Almén, K. Maqbool, M. Grabherr, A. Martinez-Barrio, M. Promerová, C.-J. Rubin, C. Wang, N. Zamani, B. R. Grant, P. R. Grant, M. T. Webster, L. Andersson, Evolution of Darwin's finches and their beaks revealed by genome sequencing. *Nature* **518**, 371–375 (2015).
6. M. J. West-Eberhard, *Developmental Plasticity and Evolution* (Oxford Univ. Press, Oxford, 2003), 816 pp.
7. E. O. Wilson, The origin and evolution of polymorphism in ants. *Q. Rev. Biol.* **28**, 136–156 (1953).
8. N. A. Moran, The evolution of aphid life cycles. *Annu. Rev. Entomol.* **37**, 321–348 (1992).
9. S. M. Shuster, Alternative reproductive behavior: Three discrete male morphs in *Paracerceis sculpta*, an intertidal isopod from the northern Gulf of California. *J. Crustacean Biol.* **7**, 318–327 (1987).
10. E. Gianoli, F. Carrasco-Urra, Leaf mimicry in a climbing plant protects against herbivory. *Curr. Biol.* **24**, 984–987 (2014).
11. G. C. Martin, A. M. Owen, J. I. Way, Nematodes, figs, and wasps. *J. Nematol.* **5**, 77–78 (1973).
12. N. Vovlas, R. N. Inserra, N. Greco, *Schistonchus caprifici* parasitizing caprifig (*Ficus carica sylvestris*) florets and the relationship with its fig wasp (*Blastophaga psenes*) vector. *Nematologica* **38**, 215–226 (1992).
13. E. A. Herre, Population structure and the evolution of virulence in nematode parasites of fig wasps. *Science* **259**, 1442–1445 (1993).
14. R. M. Giblin-Davis, K. A. Davies, G. S. Taylor, W. K. Thomas, Entomophilic nematode models for studying biodiversity and cospeciation, in *Nematology, Advances and Perspectives: Nematode Morphology, Physiology and Ecology*, Z. X. Chen, S. Y. Chen, D. W. Dickson, Eds. (CABI Publishing, Wallingford, Oxfordshire, 2004), pp. 493–540.
15. N. Kanzaki, R. M. Giblin-Davis, K. Davies, W. Ye, B. J. Center, W. K. Thomas, *Teratodiplogaster fignewmani* gen. nov., sp. nov. (Nematoda: Diplogastridae) from the syconia of *Ficus racemose* in Australia. *Zool. Sci.* **26**, 569–578 (2009).
16. A. Krishnan, S. Muralidharan, L. Sharma, R. M. Borges, A hitchhiker's guide to a crowded syconium: How do fig nematodes find the right ride? *Funct. Ecol.* **24**, 741–749 (2010).
17. V. Susoy, E. J. Ragsdale, N. Kanzaki, R. J. Sommer, Rapid diversification associated with a macroevolutionary pulse of developmental plasticity. *Elife* **4**, e05463 (2015).
18. I. L. Dryden, K. V. Mardia, *Statistical Shape Analysis* (Wiley, Chichester, 1998), 376 pp.
19. P. Mitteroecker, P. Gunz, M. Bernhard, K. Schaefer, F. L. Bookstein, Comparison of cranial ontogenetic trajectories among great apes and humans. *J. Hum. Evol.* **46**, 679–698 (2004).
20. R. I. Molnar, G. Bartelmes, I. Dinkelacker, H. Witte, R. J. Sommer, Mutation rates and intraspecific divergence of the mitochondrial genome of *Pristionchus pacificus*. *Mol. Biol. Evol.* **28**, 2317–2326 (2011).
21. C. Rödelsperger, R. A. Neher, A. M. Weller, G. Eberhardt, H. Witte, W. E. Mayer, C. Dieterich, R. J. Sommer, Characterization of genetic diversity in the nematode *Pristionchus pacificus* from population-scale resequencing data. *Genetics* **196**, 1153–1165 (2014).
22. E. J. Ragsdale, M. R. Müller, C. Rödelsperger, R. J. Sommer, A developmental switch coupled to the evolution of plasticity acts through a sulfatase. *Cell* **155**, 922–933 (2013).
23. A. Cruaud, N. Rønsted, B. Chantarasuwan, L. S. Chou, W. L. Clement, A. Couloux, B. Cousins, G. Genson, R. D. Harrison, P. E. Hanson, M. Hossaert-Mckey, R. Jabbour-Zahab, E. Jousselin, C. Kerdelhué, F. Kjellberg, C. Lopez-Vaamonde, J. Peebles, Y.-Q. Peng, R. A. S. Pereira, T. Schramm, R. Ubaidillah, S. van Noort, G. D. Weiblen, D.-R. Yang, A. Yodpinyanee, R. Libeskind-Hadas, J. M. Cook, J.-Y. Rasplus, V. Savolainen, An extreme case of plant–insect codiversification: Figs and fig-pollinating wasps. *Syst. Biol.* **61**, 1029–1047 (2012).
24. G. W. Yeates, T. Bongers, R. G. M. De Goede, D. W. Freckman, S. S. Georgieva, Feeding habits in soil nematode families and genera—An outline for soil ecologists. *J. Nematol.* **25**, 315–331 (1993).
25. T. Bongers, The Maturity Index, the evolution of nematode life history traits, adaptive radiation and cp-scaling. *Plant Soil* **212**, 13–22 (1999).
26. J. D. Van Dyken, M. J. Wade, The genetic signature of conditional expression. *Genetics* **184**, 557–570 (2010).
27. D. W. Pfennig, M. A. Wund, E. C. Snell-Rood, T. Cruickshank, C. D. Schlichting, A. P. Moczek, Phenotypic plasticity's impacts on diversification and speciation. *Trends Ecol. Evol.* **25**, 459–467 (2010).
28. S. R. Purandare, R. D. Bickel, J. Jaquiery, C. Rispe, J. A. Brisson, Accelerated evolution of morph-biased genes in pea aphids. *Mol. Biol. Evol.* **31**, 2073–2083 (2014).

29. D. W. Pfennig, P. J. Murphy, How fluctuating competition and phenotypic plasticity mediate species divergence. *Evolution* **56**, 1217–1228 (2002).
30. M. R. Orr, T. B. Smith, Ecology and speciation. *Trends Ecol. Evol.* **13**, 502–506 (1998).
31. U.S. Department of Agriculture, Agricultural Research Service, *USDA National Nutrient Database for Standard Reference, Release 27. Nutrient Data Laboratory Home Page*, 2014; www.ars.usda.gov/nutrientdata
32. R. Li, H. Zhu, J. Ruan, W. Qian, X. Fang, Z. Shi, Y. Li, S. Li, G. Shan, K. Kristiansen, S. Li, H. Yang, J. Wang, J. Wang, De novo assembly of human genomes with massively parallel short read sequencing. *Genome Res.* **20**, 265–272 (2010).
33. M. Boetzer, C. V. Henkel, H. J. Jansen, D. Butler, W. Pirovano, Scaffolding pre-assembled contigs using SSPACE. *Bioinformatics* **27**, 578–579 (2011).
34. W. Xue, J.-T. Li, Y.-P. Zhu, G.-Y. Hou, X.-F. Kong, Y.-Y. Kuang, X.-W. Sun, L_RNA_scaffolder: Scaffolding genomes with transcripts. *BMC Genomics* **14**, 604 (2013).
35. H. Li, R. Durbin, Fast and accurate long-read alignment with Burrows–Wheeler transform. *Bioinformatics* **26**, 589–595 (2010).
36. M. Clement, Q. Snell, P. Walker, D. Posada, K. Crandall, TCS: Estimating gene genealogies. *Proc. 16th Int. Parallel. Distrib. Process Symp.* **2**, 184 (2002).
37. R. C. Edgar, MUSCLE: Multiple sequence alignment with high accuracy and high throughput. *Nucleic Acids Res.* **32**, 1792–1797 (2004).
38. K. Tamura, G. Stecher, D. Peterson, A. Filipski, S. Kumar, MEGA6: Molecular Evolutionary Genetics Analysis version 6.0. *Mol. Biol. Evol.* **30**, 2725–2729 (2013).
39. J. G. Baldwin, C. D. Eddleman, R. M. Giblin-Davis, D. S. Williams, J. T. Vida, W. K. Thomas, The buccal capsule of *Aduncospiculum halicti* (Nemata: Diplogasterina): An ultrastructural and molecular phylogenetic study. *Can. J. Zool.* **75**, 407–423 (1997).
40. E. J. Ragsdale, J. G. Baldwin, Resolving phylogenetic incongruence to articulate homology and phenotypic evolution: A case study from Nematoda. *Proc. Bio. Sci.* **277**, 1299–1307 (2010).
41. F. J. Rohlf, *TpsDig2: A Program for Landmark Development and Analysis* (Department of Ecology and Evolution, State University of New York at Stony Brook, Stony Brook, 2008); http://life.bio.sunysb.edu/morph/
42. C. P. Klingenberg, MorphoJ: An integrated software package for geometric morphometrics. *Mol. Ecol. Resour.* **11**, 353–357 (2011).
43. N. Navarro, MDA: A MATLAB-based program for morphospace-disparity analysis. *Comput. Geosci.* **29**, 655–664 (2003).
44. R. Floyd, E. Abebe, A. Papert, M. Blaxter, Molecular barcodes for soil nematode identification. *Mol. Ecol.* **11**, 839–850 (2002).
45. M. Herrmann, W. E. Mayer, R. J. Sommer, Nematodes of the genus *Pristionchus* are closely associated with scarab beetles and the Colorado potato beetle in Western Europe. *Zoology* **109**, 96–108 (2006).
46. A. E. Darling, G. Jospin, E. Lowe, F. A. Matsen IV, H. M. Bik, J. A. Eisen, PhyloSift: Phylogenetic analysis of genomes and metagenomes. *PeerJ* **2**, e243 (2014).
47. W. E. Mayer, M. Herrmann, R. J. Sommer, Phylogeny of the nematode genus *Pristionchus* and implications for biodiversity, biogeography and the evolution of hermaphroditism. *BMC Evol. Biol.* **7**, 104 (2007).
48. K. Katoh, D. M. Standley, MAFFT multiple sequence alignment software version 7: Improvements in performance and usability. *Mol. Biol. Evol.* **30**, 772–780 (2013).
49. F. Ronquist, M. Teslenko, P. van der Mark, D. L. Ayres, A. Darling, S. Höhna, B. Larget, L. Liu, M. A. Suchard, J. P. Huelsenbeck, MrBayes 3.2: Efficient Bayesian phylogenetic inference and model choice across a large model space. *Syst. Biol.* **61**, 539–542 (2012).
50. M. A. Miller, W. Pfeiffer, T. Schwarz, Creating the CIPRES Science Gateway for inference of large phylogenetic trees, in *Proceedings of the Gateway Computing Environments Workshop (GCE)*, 14 November 2006, New Orleans, pp. 1–8.
51. A. J. Drummond, A. Rambaut, BEAST: Bayesian Evolutionary Analysis by Sampling Trees. *BMC Evol. Biol.* **7**, 214 (2007).

Acknowledgments: We thank J. Berger for scanning electron microscopy analysis, M. Lalk for chemical analyses, and D. Strasberg, J. Rochat, J. M. Meyer, and the staff of the Office national des forêts (La Réunion) and Parc national de La Réunion for collecting permits and long-term support with sample collection. **Funding:** This work was funded by the Max Planck Society. C.N.N. was funded in part by the Vietnam National Foundation of Science and Technology (NAFOSTED) through project 106.12-2012.84. **Author contributions:** V.S., E.J.R., and R.J.S. conceived and designed the study. V.S., M.H., N.K., M.K., C.N.N., R.M.G.-D., and R.J.S. collected the samples. V.S. and N.K. acquired the data. V.S., W.R., and C.W. performed data sequencing. V.S. and C.R. analyzed the data. V.S., E.J.R., and R.J.S. wrote the manuscript. **Competing interests:** The authors declare that they have no competing interests. **Data and materials availability:** Sequences generated for this study have been deposited in GenBank under accession numbers KT188832 to KT188928. The genome assembly of *P. borbonicus* and a file with 10,509 concatenated SNPs from 49 individuals are available at www.pristionchus.org/borbonicus/. All other data needed to evaluate the conclusions in the paper are available in present in the paper and/or the Supplementary Materials. Additional data related to this paper may be requested from the authors.

Submitted 3 August 2015
Accepted 10 November 2015
Published 15 January 2016
10.1126/sciadv.1501031

Citation: V. Susoy, M. Herrmann, N. Kanzaki, M. Kruger, C. N. Nguyen, C. Rödelsperger, W. Röseler, C. Weiler, R. M. Giblin-Davis, E. J. Ragsdale, R. J. Sommer, Large-scale diversification without genetic isolation in nematode symbionts of figs. *Sci. Adv.* **2**, e1501031 (2016).